IEEE Transactions on Smart Grid, Volume 11, Issue 6, November 2020, pp. 4700-4713
DOI: 10.1109/TSG.2020.2994111

Sequential Disaster Recovery Model for Distribution Systems with Co-Optimization of Maintenance and Restoration Crew Dispatch

Gang Zhang, Feng Zhang, *Member*, *IEEE*, Xin Zhang, *Senior Member*, *IEEE*, Ke Meng, *Member*, *IEEE*, and Zhao Yang Dong, *Fellow*, *IEEE*

***Abstract*—To efficiently restore electricity customers from a large-scale blackout, this paper proposes a novel mixed-integer linear programing (MILP) model for the optimal disaster recovery of power distribution systems. In the proposed recovery scheme, the maintenance crews (MCs) are scheduled to repair damaged components, and the restoration crews (RCs) are dispatched to switch on the manual switches. Then, the MC and RC dispatch models are integrated into the disaster recovery scheme, which will generate an optimal sequence of control actions for distributed generation (DG), controllable load, and remote/manual switches. Besides, to address the time scale related challenges in the model formulation, the technical constraints for system operation are investigated in each energization step rather than time step, hence the co-optimization problem is formulated as an "event-based" model with variable time steps. Consequently, the disaster recovery, MC dispatch and RC dispatch are properly cooperated, and the whole distribution systems can be restored step by step. Last, the effectiveness of the co-optimization model is validated in the modified IEEE 123 bus test distribution system.**

***Index Terms*—Disaster recovery, distribution system, switching sequence, maintenance crew, restoration crew, resilience**

NOMENCLATURE

1) Sets and Indices

B_m	Set of branches in node cell m
DP	Set of depots
E^{MC}	Set of travel paths connecting depots and damaged components
E^{RC}	Set of travel paths connecting depots and manual switches
I , B	Sets of nodes and branches
N	Set of node cells
N^{BS}	Set of node cells containing the substation or black start DG
$n(i)$,$m(i)$	Sets of parent buses and children buses of bus i
V^{MC}	Set of crew depots and damaged components
V_m^{MC}	Set of damaged components in the cell m
V^{MSW}	Set of manual switches
V_a^{MSW}	Set of the manual switch at vertex a
V^{RC}	Set of crew depots and manual switches
V^{RSW}	Set of remote-controlled switches
Ω_m^c	set of the loads and DGs in the node cell m
T	Set of the energization time t_c
Υ	Set of switchable loads and DGs
a,b	Indices for vertices in graph G^{RC} (V^{RC}, E^{RC})
c	Index for loads and DGs
dp	Index for depots
$dp(mc)$	Index for the depot where the mc travels starting and returning.
$dp(rc)$	Index for the depot where the rc travels starting and returning.
i,j	Indices for nodes
k,l	Indices for vertices in graph G^{MC} (V^{MC}, E^{MC})
m,n	Indices for node cells
mc	Index for maintenance crews
rc	Index for restoration crews
t	Index for time

2) Parameters

M	The large number used in linearization method
P_i^L	Active loads at bus i
P_i^{max} , Q_i^{max}	The active and reactive power limits of DG at bus i
$P_{i,j}^{max}$,$Q_{i,j}^{max}$	The active and reactive power limits of line ij
$R_{i,j}$,$X_{i,j}$	The resistance and reactance of line ij
T_c	Energization time delay for the switchable load or DG c
$T_{a,rc}^{MSW}$	The time needed by the crew rc to close the manual switch at vertex a
$T_{k,mc}^{RP}$	The time needed by the crew mc to repair the the component at vertex k
$T_{m,n}^{RSW}$	The operating time of the remote-controlled switch connecting m and n
$T_{a,b,rc}^{TRA}$	The required time of the crew rc to travel from the vertex a to b
$T_{k,l,mc}^{TRA}$	The required time of the crew mc to travel from the vertex k to l
U_0	The reference voltage magnitude

G. Zhang and F. Zhang are with the Key Laboratory of Power System Intelligent Dispatch and Control, Ministry of Education, Shandong University, Jinan, 250061, China (e-mail: fengzhang@sdu.edu.cn).

X. Zhang is with the Energy and Power Theme, School of Water, Energy and Environment, Cranfield University, Cranfield MK43 0AL, U.K. (e-mail:, xin.zhang@cranfield.ac.uk).

K. Meng and Z. Y. Dong are with the School of Electrical Engineering and Telecommunications, The University of New South Wales, NSW 2052, Australia (e-mail: kemeng@ieee.org, zydong@ieee.org).

U_i^{max} ,U_i^{min} The maximum and minimum voltage magnitudes at bus i

ϕ^L The power factor for load

ω_i The priority weight of the load at node i

ε The small number used in linearization method

2) Decision Variables

A_m^{DRM} The time when the node cell m is energized

$A_{k,mc}^{MC,AR}$ The time when the crew mc arrives at the damaged component at vertex k

$A_k^{MC,RP}$ The time when the reparation for the damaged component at vertex k is accomplished

$A_{a,rc}^{RC,AR}$ The time when the crew rc arrives at the manual switch at vertex a

$A_a^{RC,MSW}$ the time when the manual switch at vertex a is closed

$A_{m,n}^{RSW}$ The closing time of the remote-controlled switch connecting m and n

$P_{i,j,t}$,$Q_{i,j,t}$ Active and reactive power flow of line ij at time t

$P_{i,t}^g$, $Q_{i,t}^g$ Active and reactive power output of DGs at bus i and time t

t_c The energization time of component c

t_i^L The energization time of the load at node i

$x_{m,n}^{DRM}$ Binary variable indicating whether the switchable line between node cell m and n is closed and energized with m preceding n

$x_{c,t}^{EGS}$ Binary variable indicating the energization statuses of the component c at time t

$x_{i,j,t}^{EGS}$ Binary variable indicating the energization statuses of the line ij at time t

$x_{i,t}^{EGS,L}$, $x_{i,t}^{EGS,G}$ the energization statuses of loads and DGs at node i and time t

$x_{m,n,t}^{EGS}$ Binary variable indicating the energization statuses of the switchable line mn at time t

$x_{k,l,mc}^{MC}$ Binary variable indicating whether a maintenance crew mc travels from the vertex k to l.

$x_{a,b,rc}^{RC}$ Binary variable indicating whether a crew rc travels from the vertex a to b

4) Acronyms

AMI	Advanced metering infrastructure
CIS	Customer information system
DG	Distributed generator
DRM	Disaster recovery model
GIS	Geographic information system
MC	Maintenance crew
MCDM	Maintenance crew dispatch model
MILP	Mixed-integer linear programing
OMS	Outage management system
PRFI	Protective relays and fault indicator
RC	Restoration crew
RCDM	Restoration crew dispatch model
SCADA	Supervisory control and data acquisition

I. Introduction

Power distribution systems are often vulnerable to natural disasters due to the fragile energy infrastructure. For example, in 2017, Hurricane Harvey and Irma damaged massive facilities in power distribution systems leading to the interrupted power supply to nearly 300 thousand homes [3] and 15 million customers [4]. The importance of protecting power distribution systems from catastrophes has been highlighted by researchers [1], and a series of measures have been taken by utilities to enhance the system resilience [2]. Consequently, it is critical to design an effective disaster recovery model for the power distribution systems to restore customers from power outages in a timely manner.

In particular, a feasible disaster recovery model (DRM) aims to integrate maintenance crew dispatch model (MCDM) and restoration crew dispatch model (RCDM) to reflect the role and impacts of repair crews in system restoration. The interrelation and interdependence of DRM, MCDM and RCDM are proposed in Fig. 1. The restoration of a fault zone will depend on the repair time of damaged components that is highly dependent on maintenance crew (DRM couples with MCDM). The energization to a manually switched feeder is constrained by the arrival time of restoration crews (DRM couples with RCDM). In addition, if a fault zone is energized by manual switches, these switches will require to be remain open for the isolation of damaged components until being repaired (MCDM couples with RCDM). Hence, it is essential to co-optimize these models to improve the service restoration. However, the interdependence of DRM, MCDM and RCDM has not been comprehensively studied in the existing research. For example, common restoration models only considered the efficient utilization infrastructure and facilities in distribution systems, e.g., microgrids [5]-[6], dispatchable DGs [7], renewable energy [8] and transportable energy storage [9]. Although these studies have significantly contributed to the service restoration of distribution systems, the interrelation of maintenance and restoration crews with MCDM and RCDM may deteriorate the feasibility and optimality of the restoration solution. Consequently, some work has been conducted to integrate the maintenance crew (MC) dispatch [10]-[13] and manual switch operation [14] into the DRM. In [10], a MC routing model was formulated and embedded into the disaster recovery problem of distribution systems. Further, the uncertainty of repair time was considered, and a two-stage service restoration model was designed in [11]. In [12], the service restoration model of distribution systems was cooperated with the MC and mobile power source dispatch simultaneously. In [13], a pre-hurricane repair team placement model was proposed to reduce the outage duration and costs of electricity interruption in distribution systems. In [14], the different operation timescales of remote-controlled and manual switches were investigated in the DRM, but the restoration crew (RC) routing problem that leads to the time scale difference was not considered. It can be seen that the interrelation of DRM, MCDM and RCDM has not been fully investigated, and the co-optimization of these restoration models remain unsolved.

In addition to the coordination of DRM, MCDM and RCDM, a practical distribution system restoration model is also required

to generate the final configuration of the restored network, along with a step by step switching sequence towards this configuration [15]. However, most of existing studies only focused on the final configuration from the DRM model [7]-[12], which will result in final configuration infeasible if any constraints violation made during the switching stages. Therefore, several research attempted to integrate the switching sequence into the DRM model, solving by heuristic methods (e.g., tabu search method [16], fuzzy algorithm [17], and expert system [18]) and mathematical optimization (e.g., MILP in references [14], [19] and [20]). These studies have made considerable progress in generating the switching sequence for the independent DRM. However, when the DRM, MCDM and RCDM are co-optimized, new challenges have arisen to obtain the optimal configuration and corresponding switching sequence. For example, the manual switch operation is constrained by the RC routing problem; and the different time scales of DRM, MCDM and RCDM need to be addressed because employing small time steps for solution will increase the computational burden, whereas using large time steps for solution will render an inefficient solution [19].

In this paper, three research questions in designing and co-optimizing restoration models are addressed: 1) How to formulate the DRM, MCDM and RCDM. and the interdependence of these models; 2) how to address the different time scales of DRM, MCDM and RCDM in the disaster recovery process, and 3) how to effectively solve and co-optimize the proposed models. The main contributions of this paper are summarized as follows.

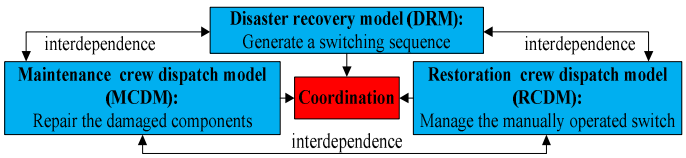

Fig.1. Interrelation among DRM, MCDM and RCDM.

To conclude, designing this co-optimization model has difficulties mainly in three aspects: 1) How to formulate the DRM, MCDM, RCDM and the interdependence among these models; 2) how to address the different time scales of DRM, MCDM and RCDM, and 3) how to promptly solve this co-optimization model. To bridge these research gaps, a co-optimization model coordinating the DRM, MCDM and RCDM is proposed in this paper Summarily, the main contributions of this paper are enumerated as follows.

1) A novel DRM-MCDM-RCDM co-optimization model is proposed, where the DRM, MCDM and RCDM are modelled and integrated by investigating their interrelation and interdependency.

2) The co-optimization problem is formulated as an "event-based" model that is dependent on system operational constraints in energization steps. The model is flexible and variable in time steps rather than having a fixed time step for the whole model.

3) The "Big-M" and "Small-ε" based linearization techniques are proposed, together with the clustering methods to pre-process the co-optimization model for the reduction of computational burden. Therefore, the optimal system configuration and switching sequence can be effectively obtained and be compatible with the solvers.

The remaining paper is organized as follows. The mathematical formulation of the co-optimization model is proposed in Section II. The linearization and clustering methods are presented in Section III. The numerical test is performed in Section IV. The conclusion is drawn in Section V.

II. Mathematical Formulation

In this section, the methodology to propose the DRM-MCDM-RCDM co-optimization model is firstly introduced in Section II-A, then the mathematical formulations of MCDM, RCDM and DRM are presented in Section II-B, II-C and II-D, respectively. Last, the interdependence of sub-models is addressed in Section II-E, and key factors such as objective function, constraints, data uncertainty and errors of co-optimization model are discussed in Section II-F.

A. Methodology

As shown in Fig. 2, to recover the multiple faults in distribution systems caused by a natural disaster, the outage management system (OMS) will firstly collect data based on the situational awareness of various information systems including supervisory control and data acquisition (SCADA) system, customer information system (CIS), geographic information system (GIS), advanced metering infrastructure (AMI), protective relays and fault indicators (PRFI) and the reports from the on-site crews [20]. It is worth mentioning that the sufficient information from situational awareness systems is critical for the fault location determination and isolation, damage assessment, system state identification and service restoration. Then, based on the collected information, the fault components are located and isolated by switching off the corresponding switches. After that, the damage assessment is conducted to estimate the repair time, and subsequently the available resources for service restoration are determined by the system state identification, such as the availability of DGs, MCs and RCs. Last, the proposed DRM-MCDM-RCDM co-optimization model is used to effectively dispatch the MCs and RCs, and generate the optimal sequence of control actions for DGs, controllable loads, and remotely/manually operated switches.

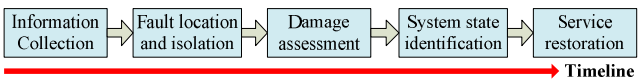

Fig.2. Framework of the proposed disaster recovery methodology.

B. Maintenance Crew Dispatch Model

The MCDM is an essential part of the co-optimization model, which aims to transport the MCs and repair the damaged components effectively, as a key requirement of restoring the customers in faulty zones. The MCDM can be divided into two interdependent sub-tasks of modelling: the routing task to determine the MCs' travel path, and the scheduling task to set the timetable of MCs' repair work [12].

In the MC routing problem, let V^{MC} and E^{MC} denote the set of vertices and edges in undirected graph $G^{MC}(V^{MC}, E^{MC})$. The vertices (denoted as k and l) in graph contain the depots (denoted

as *dp*) and damaged components. The edges in graph represent the available travel paths connecting two vertices. Let the binary variable $x^{MC}_{k,l,mc}$ denote whether a maintenance crew *mc* travels from the vertices *k* to *l*. The binary variable $x^{MC}_{k,l,mc}$ equals 1 if *mc* travels from *k* to *l*, and 0 otherwise. According to these definitions, the MC routing problem can be formulated as follows.

Each maintenance crew *mc* travels in graph G^{MC} starting from a depot *dp*(*mc*) and returning to the same depot. Moreover, the *mc* will not travel to the depots expect for *dp*(*mc*), i.e., :

$$\begin{cases} \sum_k x^{MC}_{dp(mc),k,mc}=\sum_k x^{MC}_{k,dp(mc),mc}=1, & \forall mc \\ \sum_k x^{MC}_{dp,k,mc}=\sum_k x^{MC}_{k,dp,mc}=0, & \forall mc,\ \forall dp\in DP\ /\ \{dp(mc)\} \end{cases} \tag{1}$$

For each *mc* arriving at the vertex *k*, the *mc* will leave *k* and move to the next vertex, which means:

$$\sum_l x^{MC}_{k,l,mc}=\sum_l x^{MC}_{l,k,mc}\le 1,\quad \forall mc,\ \forall k\in V^{MC}/DP \tag{2}$$

Each damaged component is repaired by one *mc*, hence:

$$\sum_{mc}\sum_l x^{MC}_{l,k,mc}=1,\ \forall k\in V^{MC}/DP \tag{3}$$

In the MC scheduling problem, let $A^{MC,AR}_{k,mc}$ denote the time when the crew *mc* arrives at vertex *k*, and let $A^{MC,RP}_{k}$ denote the time when the repair work for the damaged component at vertex *k* is completed. Then, let be the expected time needed by the crew *mc* to repair the component at vextex *k*, and let $T^{TRA}_{k,l,mc}$ be the required time of the crew *mc* to travel from the vertex *k* to *l*. It is noted that the value of $T^{RP}_{dp,mc}$ is set as 0. Let M denote a large number that is used in model formulation and linearization. Under these definitions, the MC scheduling problem can be modeled as follows.

If a crew *mc* travels from the vertex *k* to *l* (i.e., $x^{MC}_{k,l,mc}=1$), the crew *mc* will arrive at vertex *l* at time $A^{MC,AR}_{l,mc}=A^{MC,AR}_{k,mc}+T^{RP}_{k,mc}+T^{TRA}_{k,l,mc}$. This constraint can be formulated as:

$$\begin{cases} A^{MC,AR}_{l,mc}\le A^{MC,AR}_{k,mc}+T^{RP}_{k,mc}+T^{TRA}_{k,l,mc}+(1-x^{MC}_{k,l,mc})\cdot M,\ \forall mc,\forall k,l\in V^{MC} \\ A^{MC,AR}_{l,mc}\ge A^{MC,AR}_{k,mc}+T^{RP}_{k,mc}+T^{TRA}_{k,l,mc}-(1-x^{MC}_{k,l,mc})\cdot M,\ \forall mc,\forall k,l\in V^{MC} \end{cases} \tag{4}$$

For each vertex, the relationship between the $A^{MC,AR}_{k,mc}$ and $A^{MC,RP}_{k}$ can be modeled as shown in (5).

$$A^{MC,RP}_{k}=\sum_{mc}(A^{MC,AR}_{k,mc}+T^{RP}_{k,mc}\cdot\sum_l x^{MC}_{l,k,mc}),\quad \forall k\in V^{MC} \tag{5}$$

In the equation (5), if a crew *mc* is not dispatched to repair the component at vertex *k*, the value of $A^{MC,AR}_{k,mc}$ is set as 0, i.e.,:

$$0\le A^{MC,AR}_{k,mc}\le M\cdot\sum_l x^{MC}_{l,k,mc},\quad \forall mc,\forall k\in V^{MC} \tag{6}$$

In the MC routing problem, there can be a case that some MCs are not assigned repair tasks when there are more MCs than damaged components. In this case, if we define $k\neq l$, all MCs will be assigned repair tasks and dispatched from the depot *dp*(*mc*) to other vertices according to Eq. (1). Moreover, at least one damaged component will be visited by two MCs, thereby being in conflict with Eq. (3). Hence, the definition of $k\neq l$ can render the restoration model infeasible in this case.

Instead, we do not define $k\neq l$ in the MC routing problem, and the restoration model can enforce "$x^{MC}_{k,k,mc}=1$" only for the MCs with no repair task and $k=dp(mc)$ by the strategical parameter setting. Specifically, **if a *mc* is assigned the repair tasks**, the solution$x^{MC}_{k,k,mc}=1$ can serve as the alternative which indicates that the vertex *k* is visited by the crew *mc*. To avoid this solution, the value of $T^{TRA}_{k,l,mc}(\forall k\in V^{MC})$ is set to be a large number. In this case, the solution $x^{MC}_{k,k,mc}=1$ will lead to more time delay for the reparation and more load curtailments. Hence, the restoration model will generate the solution where $x^{MC}_{k,k,mc}=0$. Then, **if a *mc* is not assigned the repair tasks**, we can obtain $x^{MC}_{k,l,mc}=0$ $(\forall k,l\in V^{MC}/DP)$, certainly $x^{MC}_{k,k,mc}=0$ $(\forall k\in V^{MC}/DP)$, according to the definition for the variable $x^{MC}_{k,l,mc}$. Moreover, since the *mc* is not dispatched from the depot *dp*(*mc*) to other vertices, we can obtain $x^{MC}_{dp(mc),k,mc}=0$ $(\forall k\in V^{MC}/\{dp(mc)\})$. In further, according to Eq. (1), $x^{MC}_{dp(mc),dp(mc),mc}=1$ can be obtained in the solution in this case. Consequently, the value of $x^{MC}_{dp(mc),dp(mc),mc}$ can be used to indicate whether a *mc* is assigned the repair task or not in the proposed restoration model.

C. Restoration Crew Dispatch Model

After multiple faults in distribution systems, the remotely and manually controlled switches need to be operated coordinately to promptly restore the customers. However, the dispatch of RCs for manual switches takes time varying from minutes to hours, which is much longer than the time to operate the remote-controlled switches. Moreover, it is uneconomical and impractical to replace all manual switches with remote-controlled switches [21]. Consequently, an efficient RCDM plays an important role in the service restoration of distribution systems considering both types of switches.

The RCDM contains two interdependent sub-tasks, i.e., the RC routing problem and the RC scheduling problem. In the RC routing problem, the undirected graph $G^{RC}(V^{RC}, E^{RC})$ is first defined. In this graph, vertices (denoted as *a* and *b*) contain the depots (denoted as *dp*) and manual switches, and edges represent the available travel paths connecting two vertices. Also, the binary variable $x^{RC}_{a,b,rc}$ is introduced to indicate whether a crew *rc* travels from the vertex *a* to *b*. The binary variable $x^{RC}_{a,b,rc}$ equals 1 if *rc* travels from *a* to *b*, and 0 otherwise. Then, the RC routing problem can be formulated as follows.

$$\begin{cases} \sum_a x^{RC}_{dp(rc),a,rc}=\sum_a x^{RC}_{a,dp(rc),rc}=1, & \forall rc \\ \sum_a x^{RC}_{dp,a,rc}=\sum_a x^{RC}_{a,dp,rc}=0, & \forall rc,\ \forall dp\in DP\ /\ \{dp(rc)\} \end{cases} \tag{7}$$

$$\sum_b x^{RC}_{a,b,rc}=\sum_b x^{RC}_{b,a,rc}\le 1,\quad \forall rc,\ \forall a\in V^{RC}/DP \tag{8}$$

$$\sum_{rc}\sum_b x^{RC}_{b,a,rc}\le 1,\ \forall a\in V^{RC}/DP \tag{9}$$

Constraint (7) denotes that each restoration crew *rc* travels from a depot *dp*(*rc*) and returning to the same depot. Moreover, the *rc* will not travel to the depots expect for *dp*(*rc*). Constraint (8) indicates that once a crew *rc* closes the manual switch at vertex *a*, he will move to the manual switch at the next vertex *b*. Constraint (9) represents that a manual switch at vertex *a* can be operated by one crew only. It is noted that the definitions of constraints (7) and (8) are similar to those of (1) and (2). However, the constraint (3) is not mapped to (9), because the resto-

ration of the whole distribution system can be achieved by closing only part of manual/remote switches, hence, only part of manual switches need to be attended by RCs.

In the RC scheduling problem, $A_{a,rc}^{RC,AR}$ is introduced to represent the time when the crew *rc* arrives at the manual switch at vertex *a*, and $A_a^{RC,MSW}$ denotes the time when the manual switch at vertex *a* is closed. Then, $T_{a,rc}^{MSW}$ denotes the time of the crew *rc* to close the manual switch at vertex *a*, and $T_{a,b,rc}^{TRA}$ represents the required time of the crew *rc* to travel from *a* to *b*. It is noted that the value of $T_{a,rc}^{MSW}$ is set as 0. Based on these definitions, the RC scheduling problem can be formulated as follows.

If the manual switch at vertex *a* is closed by a crew *rc* at time $A_a^{RC,MSW}$, he or she will spend $T_{a,b,rc}^{TRA}$ time traveling from *a* to *b*, and arriving at *b* at time $A_{b,rc}^{RC,AR}$, which means:

$$\begin{cases} A_{b,rc}^{RC,AR} \le A_a^{RC,MSW} + T_{a,b,rc}^{TRA} + (1 - x_{a,b,rc}^{RC}) \cdot \mathrm{M}, & \forall rc, \forall a,b \in V^{RC} \\ A_{b,rc}^{RC,AR} \ge A_a^{RC,MSW} + T_{a,b,rc}^{TRA} - (1 - x_{a,b,rc}^{RC}) \cdot \mathrm{M}, & \forall rc, \forall a,b \in V^{RC} \end{cases} \tag{10}$$

For each vertex *a*, the relationship between $A_{a,rc}^{RC,AR}$ and $A_a^{RC,MSW}$ is formulated as (11).

$$A_a^{RC,MSW} \ge \sum_{rc} (A_{a,rc}^{RC,AR} + T_{a,rc}^{MSW} \cdot \sum_b x_{b,a,rc}^{RC}) - \mathrm{M} \cdot (1 - \sum_{rc} \sum_b x_{b,a,rc}^{RC}), \quad \forall a \in V^{RC} \tag{11}$$

It can be seen that, the formulation of (11) is different from (5) in two aspects. First, all damaged components need to be repaired, but only part of manual switches need to be visited by RCs since only part of manual/remote switches can restore the whole system. Hence, the binary $x_{b,a,rc}^{RC}$ is introduced into (11) to represent whether the switch at vertex *a* needs attending. Second, as depicted in Fig. 3a and Fig. 3b, constraint (5) is limited as an equation for $A_k^{MC,RP}$, but constraint (11) is relaxed as a range for $A_a^{RC,MSW}$ because the value of $A_a^{RC,MSW}$ is constrained by both RCDM and DRM. Therefore, RCDM only provides a feasible time interval for closing the manual switches (i.e., constraint (11)), and the accurate $A_a^{RC,MSW}$ will be finally determined by the DRM.

Besides, similar to (6), if a manual switch at vertex *a* is not visited and closed by a crew *rc*, the value of $A_{a,rc}^{RC,AR}$ is set to 0, i.e.,:

$$0 \le A_{a,rc}^{RC,AR} \le \mathrm{M} \cdot \sum_b x_{b,a,rc}^{RC}, \quad \forall rc, \forall a \in V^{RC} \tag{12}$$

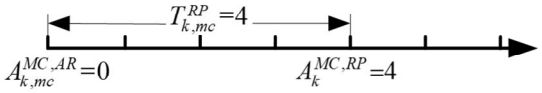

Fig. 3a. Maintenance for component *k*.

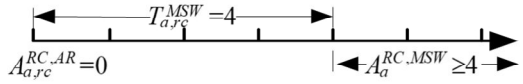

Fig. 3b. Operation for the manual switch at vertex *a* .

Similarly, we do not define $a \neq b$ in the RC routing problem, and the restoration model can enforce "$x_{a,a,mc}^{RC}=1$" only for the RCs with no task of closing manual switches and $a=dp(rc)$ by setting $T_{a,a,rc}^{TRA}(\forall a \in V^{RC})$ to a large number.

D. Disaster Recovery Model

In this paper, the DRM generates the switching sequence to energize the distribution system step by step, and dispatches the DGs sequentially to restore the customers. Correspondingly, the DRM is formulated as two interdependent sub-problems of modelling: the first task is to determine the energization path and timetable as shown in Section II-D-1, and the second task is to dispatch the DGs and checking the technical constraints in each energization step as shown in Section II-D-2.

1) Energization path and timetable

In this section, the energization path and timetable are modeled, and the energization status of components in energization steps are determined.

Energization path. Energization path is defined as follows. A node cell is defined as a cluster of nodes which are connected by non-switchable lines, such as *node cell 1* in Fig. 4. A binary variable $x_{m,n}^{DRM}$ is introduced for each switch, $x_{m,n}^{DRM}=1$ represents that the switchable line between node cell *m* and *n* is closed and energized from *m* to *n*. For example, in Fig.4, the node cells are energized with the sequence of 1→2 →3, hence, $x_{1,2}^{DRM}=x_{2,3}^{DRM}=1$, and $x_{2,1}^{DRM}=x_{3,2}^{DRM}=0$. Moreover, let *N* denote as the set of node cell, and N^{BS} denote as the set of specific node cells that contains the substation or black start DG. Based on these definitions, the energization path is modeled as follows.

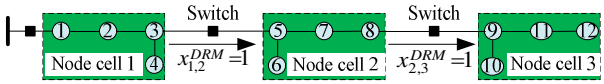

Fig.4. An example of the node cell and energization path.

An energization path starts from a node cell $m \in N^{BS}$, and should not go through the node cell $m \in N^{BS}$ to avoid the loop:

$$\sum_n x_{n,m}^{DRM} = 0, \quad \forall m \in N^{BS} \tag{13}$$

Each cell $m \in N/N^{BS}$ should be visited by one energization path to energize all cells and make the network operate radially:

$$\sum_n x_{n,m}^{DRM} = 1, \quad \forall m \in N/N^{BS} \tag{14}$$

Energization timetable. First, the energization time of node cells is determined. Let A_m^{DRM} and A_n^{DRM} denote the time when the node cell *m* and *n* are energized, respectively. Let $T_{m,n}^{RSW}$ denote the operating time of the remote-controlled switch connecting *m* and *n*. and let V^{MSW} and V^{RSW} be the set of manual and remote-controlled switches, respectively. Let $A_{m,n}^{RSW}$ be the closing time of the remote-controlled switch connecting *m* and *n*. Consequently, if a remote-controlled switch is installed on the line between *m* and *n*, A_n^{DRM} is determined by (15a), and $A_{m,n}^{RSW}$ is constrained by (15b).

$$A_{m,n}^{RSW} - \mathrm{M} \cdot (1 - x_{m,n}^{DRM}) \le A_n^{DRM} \le A_{m,n}^{RSW} + \mathrm{M} \cdot (1 - x_{m,n}^{DRM}), \forall (m,n) \in V^{RSW} \tag{15a}$$

$$A_{m,n}^{RSW} \ge A_m^{DRM} + T_{m,n}^{RSW} - \mathrm{M} \cdot (1 - x_{m,n}^{DRM}), \forall (m,n) \in V^{RSW} \tag{15b}$$

In Eq (15b), the left and right sides are unequal for two reasons. First, the value of $A_{m,n}^{RSW}$ is constrained by the binary variable $x_{m,n}^{DRM}$, i.e., whether the switchable line between *m* and *n* is energized from *m* to *n* or not during the restoration process. Specifically, if $x_{m,n}^{DRM}=0$, the relationship between $A_{m,n}^{RSW}$ and $A_m^{DRM}+T_{m,n}^{RSW}$ should be relaxed, and it can be achieved by $A_{m,n}^{RSW} \ge A_m^{DRM} + T_{m,n}^{RSW} - \mathrm{M}$ according to Eq (15b). If $x_{m,n}^{DRM}=1$, it can be obtained from Eq (15b) that $A_{m,n}^{RSW} \ge A_m^{DRM} + T_{m,n}^{RSW}$. However, the proposed model

aims to minimize the load curtailments. In this case, the model can enforce the value of $A_{m,n}^{RSW}$ to be identical to $A_m^{DRM} + T_{m,n}^{RSW}$, to reduce the outage duration of cell n if the cell n can be energized at time $A_m^{DRM} + T_{m,n}^{RSW}$. The second reason is related to the reparation for the damaged components in cell n. Specifically, If $x_{m,n}^{DRM}$ =1, the switchable line between m and n should be closed after the damaged components in cell n have been repaired. Hence, if the value of the reparation time for damaged components in cell n is larger than the value of $A_m^{DRM} + T_{m,n}^{RSW}$, the cell n cannot be energized at time $A_m^{DRM} + T_{m,n}^{RSW}$. In this case, the value of $A_{m,n}^{RSW}$ should be formulated as $A_{m,n}^{RSW} \geq A_m^{DRM} + T_{m,n}^{RSW}$ instead of $A_{m,n}^{RSW} = A_m^{DRM} + T_{m,n}^{RSW}$, as we modeled in Eq. (15b).

Similarly, if a manual switch at vertex a is installed on the line between m and n, the energization time of cell n is determined by (16a), and the closing time of the manual switch at vertex a is constrained by (16b).

$$A_a^{RC,MSW} - M(1-x_{m,n}^{DRM}) \leq A_n^{DRM} \leq A_a^{RC,MSW} + M(1-x_{m,n}^{DRM}), \forall a \in V^{MSW} \quad (16a)$$

$$A_a^{RC,MSW} \geq A_m^{DRM} + \sum_{rc} T_{a,rc}^{MSW} \cdot \sum_{b} x_{b,a,rc}^{RC} - M \cdot (1-x_{m,n}^{DRM}), \forall a \in V^{MSW} \quad (16b)$$

It is noted that equations (16a)-(16b) serve as the coupling constraints of RCDM and DRM. Specifically, in RCDM, constraint (11) defines a time range as feasible time interval for closing the manual switch at vertex a, and in DRM, the accurate time, i.e., $A_a^{RC,MSW}$, will be determined by the (16). An example of timeline to close the manual switches is shown in Fig. 5.

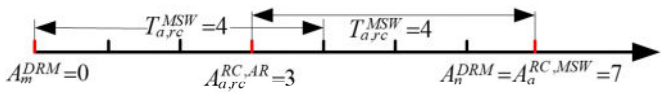

Fig.5. An example of determining the timeline of closing manual switches.

Then, the energization time of loads and DGs is determined. Let t_c be the energization time of component c. Let T be the set of t_c. For example, in Fig.4, if the energization time of the loads at node 1, 2, …, and 12 is t_1, t_2, …, and t_{12}, respectively, T is defined as $\{t_1, t_2, \ldots, t_{12}\}$. Let Υ be the set of all switchable loads and DGs in distribution systems. Moreover, we define Ω_m^c as the set of loads and DGs in the node cell m. Subsequently, t_c can be modeled as follows.

If the node cell m is energized at time A_m^{DRM}, the switchable loads and DGs in the cell m can be energized after the time delay of T_c, as modeled in (17). It is worth mentioning that the time delay denotes the switch operation time (manually or remote-controlled) for the switchable loads, and synchronization time for the DGs, respectively.

$$t_c \geq A_m^{DRM} + T_c, \quad \forall m \in N, \forall c \in \Omega_m^c \ \mathrm{I} \ \Upsilon \quad (17)$$

Eq (17) indicates that the energization to the switchable loads and DGs in cell m can be later than the energization to cell m due to the operational constraints, such as the power balance. For example, the node cell m can be energized at t=100min, and the time delay of the switchable loads and DGs in cell m is set to be 1min and 10min, respectively. Consider a case that the remaining power capacity is not enough to energize all switchable loads in cell m at t=101min, due to the power capacity limits of the substation. However, when the DGs in cell m are energized at t=110min, the power capacity is enough to energize all loads in cell m. In this case, the energization time of the switchable loads in cell m is constrained by the operational constraints, hence the energization time should be modeled as an unequal formulation, i.e., Eq (17). Moreover, if all loads can be energized at t=101min, the unequal formulation of Eq (17) is also workable because the restoration model can enforce the energization time of switchable loads to be 101min to reduce the load curtailments.

For the non-switchable load c in cell m, the load will be energized immediately when the cell m is energized, i.e., :

$$t_c = A_m^{DRM}, \quad \forall m \in N, \forall c \in \Omega_m^c / \Upsilon \quad (18)$$

Energization status. The operating conditions of distribution systems are changed when the loads or DGs are energized. Therefore, it is unnecessary to check the technical constraints in each time step. In this paper, the energization statuses of loads and DGs (19), remote-controlled switchable lines (20), manually switchable lines (21) and non-switchable lines (22) at energization steps $t_c \in \mathrm{T}$ are determined, and the technical constraints are only checked at $t_c \in \mathrm{T}$ instead of all time steps. The difference between time step and energization step is shown in Fig. 6. Energization step is defined as a time step when loads or DGs are energized. Consequently, the different time scales of DRM, MCDM and RCDM is well coordinated, and the co-optimization method is formulated as an "event-based" and variable time-step model.

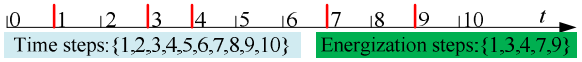

Fig.6. Comparison between time step and energization step.

First, a binary variable $x_{c,t}^{EGS}$ is defined as the energization status of component c (i.e., loads and DGs) at time $t \in \mathrm{T}$, and its value is determined by comparing t with t_c. That is:

$$x_{c,t}^{EGS} = \begin{cases} 0, & if \quad t < t_c \\ 1, & if \quad t \geq t_c \end{cases} \quad (19)$$

Then, a binary variable $x_{m,n,t}^{EGS}$ is defined as the energization status of the switchable line mn at time $t \in \mathrm{T}$. The value of $x_{m,n,t}^{EGS}$ can be determined by (20) if cell m and n are connected by a remote-controlled switch, and determined by (21) if the cell m and n are connected by a manual switch.

$$x_{m,n,t}^{EGS} = \begin{cases} 0, & if \ x_{m,n}^{DRM} = x_{m,n}^{DRM} = 0 \\ 0, & if \ x_{m,n}^{DRM} + x_{n,m}^{DRM} = 1 \ and \ t < A_{m,n}^{RSW} \\ 1, & if \ x_{m,n}^{DRM} + x_{n,m}^{DRM} = 1 \ and \ t \geq A_{m,n}^{RSW} \end{cases}, \forall (m,n) \in V^{RSW} \quad (20)$$

$$x_{m,n,t}^{EGS} = \begin{cases} 0, & if \ x_{m,n}^{DRM} = x_{m,n}^{DRM} = 0 \\ 0, & if \ x_{m,n}^{DRM} + x_{m,n}^{DRM} = 1 \ and \ t < A_a^{RC,MSW} \\ 1, & if \ x_{m,n}^{DRM} + x_{m,n}^{DRM} = 1 \ and \ t \geq A_a^{RC,MSW} \end{cases}, \forall a \in V^{MSW} \quad (21)$$

Last, i and j are the nodes in distribution systems, and B_m is the set of branches in cell m. $x_{i,j,t}^{EGS}$ is the energization status of line ij at time $t \in \mathrm{T}$. Then, for any non-switchable line $ij \in B_m$, the energization status can be obtained from:

$$x_{i,j,t}^{EGS} = \begin{cases} 0, & if \quad t < A_m^{DRM} \\ 1, & if \quad t \geq A_m^{DRM} \end{cases}, \forall m \in N, \forall ij \in B_m, \forall t \in \mathrm{T} \quad (22)$$

2) Operational constraints

The operational constraints are formulated to dispatch DGs and guarantee the security of distribution systems at $t\in \mathrm{T}$. In this paper, the linearized DistFlow model [22] is adopted, which has been widely employed and verified in system service restoration [10], [23], [24]. Specifically, constraint (23) represents the active and reactive power balance at each node; the voltage drop across the branch is characterized by (24); constraints (25), (26) and (27) set the limits on line power flow, DG output and nodal voltage, respectively. Besides, if the load i can be restored at $t=t_i$, $x_{i,t}^{EGS}=1$ for the period $t\geq t_i$. In other words, the load i can be restored at time t_i and will stay in "energization state" for $t\geq t_i$. In this case, the value of $\sum_{t\in T} x_{i,t}^{EGS,L}$ is identical to the value of $\sum_{t\in T\ and\ t\geq t_c} 1$, which is equal to or greater than 1. However, if the load i cannot be restored during the recovery process, $x_{i,t}^{EGS}=0$" for all $t\in \mathrm{T}$. In this case, the value of $\sum_{t\in T} x_{i,t}^{EGS,L}$ becomes 0. Hence, by applying the constraint (28), all customers are guaranteed to be restored.

$$\begin{cases} \sum_{j\in m(i)} P_{i,j,t} - \sum_{j\in n(i)} P_{j,i,t} = P_{i,t}^{g} - P_i^{L}\cdot x_{i,t}^{EGS,L} \\ \sum_{j\in m(i)} Q_{i,j,t} - \sum_{j\in n(i)} Q_{j,i,t} = Q_{i,t}^{g} - P_i^{L}\cdot x_{i,t}^{EGS,L}\cdot\tan(\cos^{-1}(\phi^{L})) \end{cases} \quad \forall i\in I,\forall t\in \mathrm{T} \quad (23)$$

$$\begin{cases} U_{i,t} - U_{j,t} - (R_{i,j}P_{i,j,t} + X_{i,j}Q_{i,j,t})/U_0 \leq \mathrm{M}\cdot(1 - x_{i,j,t}^{EGS}) \\ U_{i,t} - U_{j,t} - (R_{i,j}P_{ij,t}^{s} + X_{i,j}Q_{i,j,t})/U_0 \geq -\mathrm{M}\cdot(1 - x_{i,j,t}^{EGS}) \end{cases} \quad \forall (i,j)\in B,\forall t\in \mathrm{T} \quad (24)$$

$$\begin{cases} -P_{i,j}^{\max}\cdot x_{i,j,t}^{EGS} \leq P_{i,j,t} \leq P_{i,j}^{\max}\cdot x_{i,j,t}^{EGS} \\ -Q_{i,j}^{\max}\cdot x_{i,j,t}^{EGS} \leq Q_{i,j,t} \leq Q_{ij}^{\max}\cdot x_{i,j,t}^{EGS} \end{cases} \quad \forall (i,j)\in B,\forall t\in \mathrm{T} \quad (25)$$

$$0\leq P_{i,t}^{g}\leq P_i^{\max}\cdot x_{i,t}^{EGS,G},\ 0\leq Q_{i,t}^{g}\leq Q_i^{\max}\cdot x_{i,t}^{EGS,G} \quad \forall i\in I,\forall t\in \mathrm{T} \quad (26)$$

$$U_i^{\min}\leq U_{i,t}\leq U_i^{\max} \quad \forall i\in I,\forall t\in \mathrm{T} \quad (27)$$

$$\sum_{t\in \mathrm{T}} x_{i,t}^{EGS,L}\geq 1,\forall i\in I \quad (28)$$

It is noted that other technical constraints for service restoration of distribution systems can be added in this section, such as the operation of energy storage [14], cold load pick-up [25], unbalanced distribution system [20] and transient stability and frequency deviation [5]. These constraints will have scope to be implemented into the model, dependent on the specific system recovery case studies to be considered as the future work.

E. Modelling of Interdependence

The interdependence of DRM coupling with RCDM. First, the closing time of manual switches depends on both DRM and RCDM, and this coupling constraint has been formulated in (16). Second, if a manual switch at vertex a which connects cell m and n is closed and energized, this manual switch must be visited by a rc, that is:

$$\sum_{rc}\sum_{b} x_{b,a,rc}^{RC} = x_{m,n}^{DRM} + x_{n,m}^{DRM} \leq 1,\ \forall a\in V^{MSW},\forall (m,n)\in V_a^{MSW} \quad (29)$$

The interdependence of DRM coupling with MCDM. Let V_m^{MC} be the set of damaged components in the cell m. Then, the cell m should only be energized after all damaged components in cell m are repaired, which means:

$$A_m^{DRM}\geq A_k^{MC,RP} + \sum_n T_{n,m}^{RSW}\cdot x_{n,m}^{DRM} + \sum_n T_{n,m}^{MSW}\cdot x_{n,m}^{DRM},\forall k\in V_m^{MC} \quad (30)$$

The interdependence of RCDM coupling with MCDM. If a cell m is energized by closing a manual switch at vertex a between cell m and n, this manual switch at vertex a should be closed by RCs after all damaged components in the cell m are repaired by MCs. Hence, the operation of the manual switch needs the coordination of the MCDM to repair damaged components and the RCDM to dispatch the RCs, as modelled in Eq (31). However, the operation of the remote-controlled switch is not constrained by the dispatch of RCs, i.e., the RCDM. Hence, there is no interdependence of RCDM coupling with MCDM related to the remote-controlled switch.

$$A_a^{RC,MSW} - T_a^{MSW} \geq A_k^{MC,RP} - \mathrm{M}\cdot(1 - x_{n,m}^{DRM}),\forall k\in V_m^{MC},\forall n\in N \quad (31)$$

F. Co-Optimization of Model with Data Uncertainty

The co-optimization model aims to restore all customers, and reduce the load curtailment in the restoration process. Let t_i^{L} be the energization time of the load at node i, and let ω_i be the priority and weight of the load at node i. Then, the objective function is designed to minimize the load curtailment in the recovery process:

$$\min \sum_{i\in I}\omega_i\cdot t_i^{L}\cdot P_i^{L} \quad (32)$$

and subject to the following constraints:

1) MC dispatch constraints (1)-(6) in the MCDM;
2) RC dispatch constraints (7)-(12) in the RCDM;
3) Energization path and time in the DRM (13)-(22);
4) Operational constraints in the DRM (23)-(28);
5) Constraints coupling MCDR, RCDM and DRM (29)-(31).

The data uncertainty of travelling and repair time is discussed here. The travelling time is normally estimated by GIS in the "Information Collection" stage, and the repair time is normally estimated in the "Damage Assessment" stage, both stages are before the service restoration. Hence, it is assumed those parameters are available and pre-determined in this paper. However, the uncertainty of actual travelling and repair time for crews still exists in the service restoration stage, and these uncertainties can affect the optimization and feasibility of the proposed model. In this case, the proposed model needs to be extended to address these uncertainties with the following two methods.

1.Model extension. The deterministic model can be extended to a stochastic programming problem [24] or a robust optimization problem [26]. For this purpose, the uncertainty in the service restoration process should be firstly characterized, such as the application of lognormal distribution to model the repair time [27]. Then, the deterministic model can be reformulated as a stochastic or a robust model to improve robustness of the solution to uncertainty. Last, efficient solution methods should be developed to solve the extended model.

2.Time-rolling online execution. The impact of uncertainty can be alleviated by the time-rolling online execution [28]. Spe-

cifically, the control commands generated from the off-line restoration model should be time-rolling refined based on the current uncertainty realizations. For example, assuming an original solution from the off-line model that all damaged components in a faulted area can be repaired at t=30min, and this area can be energized at t=31min (1 min for the operation time of switches). However, if some unexpected events were happened during the execution process, which would lead to the reparation repair delay of 15min. Hence, the reparation repair work has to be completed is accomplished at t=45min, and correspondingly the faulted area can be energized at t=46min based on the time-rolling online optimization.

However, the main focus of this paper is to investigate the interdependence of DRM, MCDM and RCDM with variable time scales. Hence, the uncertainty will be further investigated as future work.

The input data errors are also discussed here. The data error management is a critical part during the service restoration process due to the possible failure or malfunction of DMS and SCADA systems [29]. For example, the input data errors during the model formulation can lead to a sub-optimal or infeasible solution, such as the system parameter errors, geographic information errors and available resources information errors. Hence, effective error detection, identification and correction methods are required before the modelling of service restoration, such as the geometrical approach [30]. Moreover, the input data errors during the online execution process can cause the delay or failure of system restoration, in such way of the load metering errors or communication failure. In this case, the online execution of the proposed scheme should be cooperative with the effective state estimation [31]. By applying these methods, the proposed scheme can be improved for implementation and execution.

III. Solution Method

Solving the proposed co-optimization model is a considerable challenge due to: 1) the nonlinear constraints (19)-(22); and 2) large amounts of binary variables in the MCDM and RCDM. In order to effectively obtain the optimal solution, the "Big-M" and "Small-ε" based linearization methods are proposed in Section III-A, and the co-optimization model is pre-processed by clustering the damaged components and manual switches to depots in Section III-B.

A. Linearization Method

First, the constraints (33) and (34) are formulated to linearize (19) and (22), respectively.

$$(t-t_c+\varepsilon)/\mathrm{M}\le x_{c,t}^{EGS}\le(t-t_c+\varepsilon)/\mathrm{M}+1 \tag{33}$$

$$(t-A_m^{DRM}+\varepsilon)/\mathrm{M}\le x_{i,j,t}^{EGS}\le(t-A_m^{DRM}+\varepsilon)/\mathrm{M}+1 \tag{34}$$

where the small number ε and the large number M are employed to guarantee $x_{c,t}^{EGS}=1$ when $t\ge t_c$, and $x_{c,t}^{EGS}=0$ when $t<t_c$. It is noted that the value of ε should not change the sign of $(t-t_c)$.

Then, by employing the "Big-M" and "Small-ε", the constraints (20) and (21) can be rewritten as (35) and (36), respectively. It can be seen that if and only if $x_{m,n}^{DRM}+x_{n,m}^{DRM}=1$ together with $t\ge A_{m,n}^{RSW}$, the value of the binary variable $x_{m,n,t}^{EGS}$ is limited as 1 by the constraint (35). Hence, the constraint (35) is identical to (20). Similar analysis can be conducted for (21) and (36).

$$\begin{cases} x_{m,n,t}^{EGS}\ge(x_{m,n}^{DRM}+x_{n,m}^{DRM})\cdot(t-A_{m,n}^{RSW}+\varepsilon)/\mathrm{M} \\ x_{m,n,t}^{EGS}\le(x_{m,n}^{DRM}+x_{n,m}^{DRM})\cdot(t-A_{m,n}^{RSW}+\varepsilon)/\mathrm{M}+x_{m,n}^{DRM}+x_{n,m}^{DRM} \end{cases},\forall(m,n)\in V^{RSW} \tag{35}$$

$$\begin{cases} x_{m,n,t}^{EGS}\ge(x_{m,n}^{DRM}+x_{n,m}^{DRM})\cdot(t-A_a^{RC,MSW}+\varepsilon)/\mathrm{M} \\ x_{m,n,t}^{EGS}\le(x_{m,n}^{DRM}+x_{n,m}^{DRM})\cdot(t-A_a^{RC,MSW}+\varepsilon)/\mathrm{M}+x_{m,n}^{DRM}+x_{n,m}^{DRM} \end{cases},\forall(m,n)\in V^{MSW} \tag{36}$$

Then, equations (35) and (36) are to be linearized. First, it is worth mentioning that $(x_{m,n}^{DRM}+x_{n,m}^{DRM})$ can be treated as a binary variable according to the Equation (29), and $(t-A_{m,n}^{RSW}+\varepsilon)$ can be treated as a continuous variable. Hence, equations (35)-(36) are non-linear due to the product of the binary variable and the continuous variable. Take (35) as an example to apply the linearization method, an auxiliary variable $\beta_{m,n}$ is firstly introduced as shown in (37).

$$\beta_{m,n}=(x_{m,n}^{DRM}+x_{n,m}^{DRM})\cdot(t-A_{m,n}^{RSW}+\varepsilon) \tag{37}$$

Hence, Equation (35) can be re-formulated as a linear form (38) by integrating (37) into (35).

$$\beta_{m,n}/\mathrm{M}\le x_{m,n,t}^{EGS}\le\beta_{m,n}/\mathrm{M}+x_{m,n}^{DRM}+x_{n,m}^{DRM} \quad ,\forall(m,n)\in V^{RSW} \tag{38}$$

Furthermore, Equation (37) can be linearized with the "Big-M" method, as shown in (39). Specifically, if the value of the binary variable $(x_{m,n}^{DRM}+x_{n,m}^{DRM})$ is 0, $\beta_{m,n}=0$ according to the first equation in (39); Otherwise, $\beta_{m,n}=t-A_{m,n}^{RSW}+\varepsilon$ according to the last two constraints in (39).

$$\begin{cases} -\mathrm{M}\cdot(x_{m,n}^{DRM}+x_{n,m}^{DRM})\le\beta_{m,n}\le\mathrm{M}\cdot(x_{m,n}^{DRM}+x_{n,m}^{DRM}) \\ \beta_{m,n}\le t-A_{m,n}^{RSW}+\varepsilon+\mathrm{M}\cdot(1-x_{m,n}^{DRM}-x_{n,m}^{DRM}) \\ \beta_{m,n}\ge t-A_{m,n}^{RSW}+\varepsilon-\mathrm{M}\cdot(1-x_{m,n}^{DRM}-x_{n,m}^{DRM}) \end{cases},\forall(m,n)\in V^{RSW} \tag{39}$$

To conclude, Equation (35) is linearized to become (38) and (39), and Equation (36) can be linearized with the same method. By employing the "Big-M" and "Small-ε" based linearization methods, the proposed co-optimization model can be formulated as a MILP problem. Consequently, the optimal solution can be obtained from the proposed model with the linearization methods.

B. Clustering Method

Large amounts of binary variables exist in the co-optimization model, especially in the MCDM and RCDM. For example, it is assumed that the number of depots, MCs in each depot, and damaged components is σ_{dp}, σ_{MC} and σ_{dm}, respectively. Then, the number of binary variables $x_{k,l,mc}^{MC}$ for each crew mc is $\sigma_{dm}\cdot(\sigma_{dm}+1)$. Therefore, the total number of binary variables in the MCDM is $\sigma_{dp}\cdot\sigma_{MC}\cdot\sigma_{dm}\cdot(\sigma_{dm}+1)$, which would substantially increase the computational burden. The same analysis can be conducted for the RCDM. Consequently, it is reasonable to cluster the damaged components and manual switches to each depot [10].

First, the clustering model for the damaged components is formulated. Let $d_{dp,k}$ be the distance between the depot dp and damaged component k, and let a binary variable $x_{dp,k}^{CLU}$ denote whether k is clustered to dp. The value of $x_{dp,k}^{CLU}$ is 1 if k is clustered to dp, and 0 otherwise. Based on these definitions, the clustering model is proposed in (40)-(41).

$$\min \sum_{dp}\sum_{k} d_{dp,k}\cdot x_{dp,k}^{CLU} \tag{40}$$

$$\text{s.t.} \sum_{dp} x_{dp,k}^{CLU}=1, \forall k \in V^{MC}/\{dp\} \quad (41)$$

The objective function (40) is to assign the damaged components to the nearest depot, thereby reducing the travel time. The constraint (41) ensures that each damaged component is assigned to a depot. By clustering the damaged components, the number of binary variables can be significantly reduced. For example, it is assumed that each depot manages σ_{dm}/σ_{dp} damaged components. Then, the number of binary variables in MCDM is $\sigma_{MC}\cdot\sigma_{dm}\cdot(\sigma_{dm}/\sigma_{dp}+1)$, which is reduced by $\sigma_{dm}\cdot\sigma_{dm}\cdot\sigma_{MC}\cdot(\sigma_{dp}-1/\sigma_{dp})$ comparing to $\sigma_{dp}\cdot\sigma_{MC}\cdot\sigma_{dm}\cdot(\sigma_{dm}+1)$ before the cluster. Consequently, the clustering method can efficiently improve the computational performance.

Similarly, the clustering model for the manual switches can be formulated as shown in (42)-(43), where $d_{dp,a}$ is the distance between the depot dp and manual switch a, and the binary variable $x_{dp,a}^{CLU}$ denote whether a is clustered to dp.

$$\min \sum_{dp}\sum_{a} d_{dp,a}\cdot x_{dp,a}^{CLU} \quad (42)$$

$$\text{s.t.} \sum_{dp} x_{dp,a}^{CLU}=1, \forall a \in V^{RC}/\{dp\} \quad (43)$$

IV. Numerical Results

The proposed co-optimization model is tested in the IEEE 123 node distribution system [32]. The modelling work is conducted in GAMS 23.7 and solved using CPLEX 12.3 on a personal computer of a core i5, 3.2 GHz processor and the 4 GB RAM. In all simulation cases, the optimality gap is set as 0.01%.

A. Test System and Case Design

The tested IEEE 123 node distribution system contains 5 substations, 6 DGs, 3 depots, 5 remote-controlled switches and 11 manual switches [19]. Moreover, there are total loads of 3490 kW and critical loads of 1020 kW, and the details are shown in Table I and Fig. 7. To simulate damaged system and available resources for disaster recovery, we create a scenario with 15 branches damaged by the natural disaster, as shown in Fig. 7. Moreover, each depot contains 2 MCs, and depot 1 and depot 2 contain 1 RC, respectively.

TABLE I LOADS AND CRITICAL LOADS (CL) IN EACH NODE CELL

Node Cell	1	2	3	4	5	6	7	8	9	10	Others	Total
Loads(kW)	160	240	160	200	755	550	705	240	160	320	0	3490
CLs (kW)	0	60	80	80	290	330	0	0	0	180	0	1020

TABLE II PRE-ASSIGNMENT OF DAMAGED BRANCHES AND MANUAL SWITCHES

	Depot 1	Depot 2	Depot 3
Damaged branch	Branch 1-3, 7-8, 13-34, 18-19, 25-26	Branch 35-36, 44-47, 54-57, 57-60, 60-62	Branch 67-160, 76-86, 89-91, 101-105, 109-110
Manual switch	Switch 1-7, 13-18, 23-25, 76-77, 87-89, 13-152	Switch 18-135, 60-160, 97-197, 54-94, 151-300	——

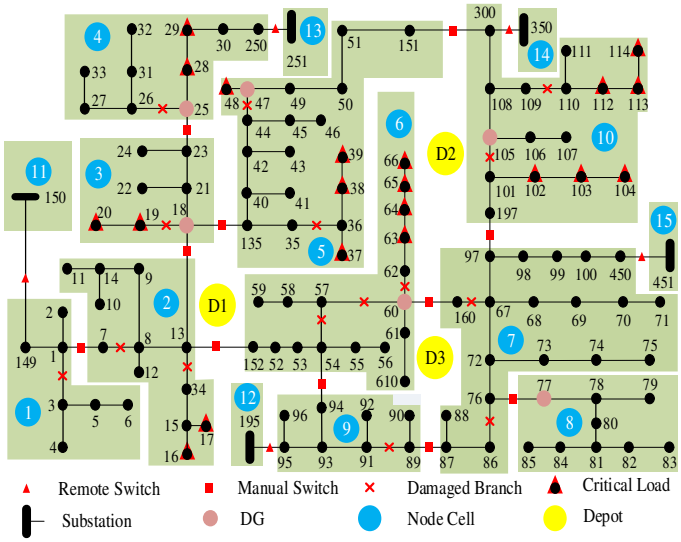

Fig.7. Modified IEEE 123 node distribution system.

First, 15 damaged branches and 11 manual switches are clustered and pre-assigned to depots based on the model (40)-(41) and (42)-(43), respectively, and the results are shown in Table III. In addition, the expected time needed by a RC to repair the damaged branch T_k^{RP} is listed in Table III, and the operating time of the manual and remote-controlled switches, is listed in Table IV. Due to the lack of real data, it is assumed that the travel time ranging from 15 min to 60 min is randomly generated in *Matlab* by using the random number generator.

TABLE III EXPECTED TIME TO REPAIR THE DAMAGED BRANCH

Branch	1-3	7-8	13-34	18-19	25-26	35-36	44-47	54-57
Time (min)	98	53	75	91	107	112	76	42
Branch	57-60	60-62	67-160	76-86	89-91	101-105	109-110	
Time (min)	43	51	120	111	94	49	101	

TABLE IV OPERATING TIME OF SWITCHES

Switch	150-149	195-95	251-250	350-300	451-450
Time (min)	1	1	1	1	1
Switch	1-7	13-18	23-25	76-77	87-89	13-152
Time (min)	8	8	10	10	9	7
Switch	18-135	60-160	97-197	54-94	151-300
Time (min)	10	8	6	11	11

B. Numerical Results

The proposed co-optimization model is solved in 782 s. The calculated travel paths of MCs and RCs are shown in Fig.8 and Fig.9, respectively, where each color represents a crew. Moreover, the arrival and departure time of MCs and RCs are listed in Table V. The energization sequence of switches, node cells, controllable loads and DGs are shown in Table VI.

By employing the proposed model, the system is optimally divided into 5 subsystems and all loads have been restored as shown in Fig. 9. In addition, as shown in Table V, the operational constraints (23)-(28) only need to be checked at "energization-based" time, e.g., t=161min (cell 4), t=165min (cell 7)

and t=171min (cell 3). Consequently, the proposed co-optimization model is "event-based" allowing variable time steps, which can efficiently address the different time scales of DRM, MCDM and RCDM.

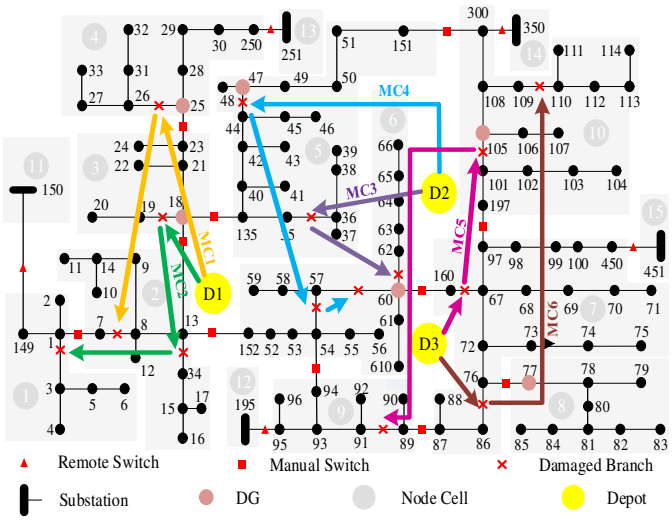

Fig. 8. Travel path of 6 maintenance crews.

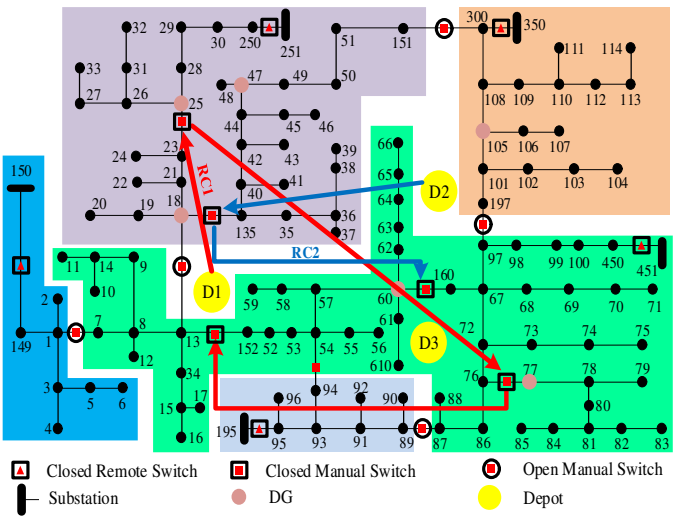

Fig.9. Energized system and the travel path of RCs.

TABLE V TRAVEL PATH OF MCS AND RCS

Depot	Crew	Travel Path [*arriving/leaving time* (min)]
Depot 1	MC1	25-26 [***53/160***] → 7-8 [***201/254***]
	MC2	18-19 [***37/128***] → 13-34 [***165/240***] → 1-3 [***255/353***]
Depot 2	MC3	35-36 [***41/153***]→60-62 [***199/250***]
	MC4	44-47 [***37/113***]→54-57 [***130/172***]→57-60 [***189/232***]
Depot 3	MC5	67-160[***44/164***]→101-105[***214/263***]→89-91[***286/380***]
	MC6	76-86 [***21/132***] → 109-110 [***161/262***]
Depot 1	RC1	23-25[***28/117***] → 76-77[***227/237***] → 13-152[***265/272***]
Depot 2	RC2	18-135[***35/181***] → 60-160[***240/258***]

TABLE VI ENERGIZATION OF SWITCHES, NODE CELLS, LOADS AND DGS

Time (min)	Energization Sequence				Restored Loads in the Event (kW)
	Switches	Node Cells	Loads in Cell-X	DGs in Node-X	
0		11,12,13,14,15			
161	250-251	4			
162			4		200
165	450-451	7			
166			7	25	705
171	23-25	3			
172			3		160
176				18	
181	18-135	5			
182			5		755
186				47	
237	76-77	8			
238			8		240
242				77	
258	60-160	6			
259			6		550
263				60	
264	300-350	10			
265			10		320
269				105	
272	13-152	2			
273			2		240
354	149-150	1			
355			1		160
381	95-195	9			
382			9		160

The coordination between MCDM, RCDM and DRM is key to generate the switching sequence for loads and DGs restoration. The energization of node cell 6 and 7 are taken as an example in Fig.10. First, the node cell 15 is energized by the substation at t=0 according to the DRM. Second, the damaged branches in node cell 7 are repaired by MC5 and MC6 at t=132min and 164min, respectively, according to the MCDM. Third, the remote-controlled switch between node 450 and 451 is closed at t=165min to energize the node cell 7 according to the DRM. The controllable loads in the node cell 7 can be energized at t=166min. Then, MC3 and MC4 are dispatched by the MCDM to repair the damaged branches in the node cell 6 at t=172min, 232min and 250min, respectively. After the repair completion, the manual switch between 60 and 160 is closed by RC2 at t= 258min according to the RCDM, and the node cell 6 can be energized by the DRM accordingly. Last, the controllable loads in the cell 6 can be energized at t=259min, and the DG at node 60 can be synchronized at t=263min. It can be seen that the energization sequence is coordinated by the MCDM, RCDM and DRM through the co-optimization process.

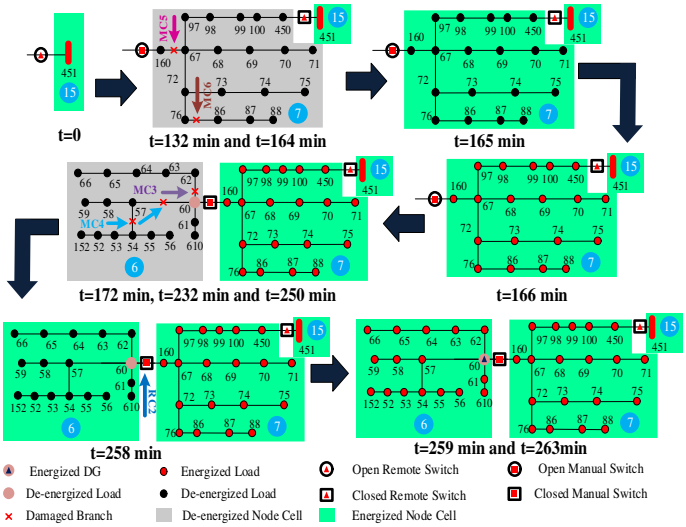

Fig.10. The sequence of control actions to energize the node cell 6

The priority of loads can affect the energization sequence, as shown in Table VII. By increasing the priority of loads, the node cells with a large number of critical loads will be energized first. For example, the energization priority of the node cell 10 with 180kW critical loads increases from 10th to 2nd, with the priority of loads increasing from 1 to 5. Moreover, a high priority weight of critical loads can lead to the less critical load shedding as shown in Table II. Therefore, the priority of loads at a node should be carefully selected to avoid the sub-optimal solution.

TABLE VII THE ENERGIZATION SEQUENCE OF NODE CELLS WITH DIFFERENT PRIORITY WEIGHTS OF CRITICAL LOADS

Priority Weight	1st	2nd	3rd	4th	5th	6th	7th	8th	9th	10th	11th	Load Shedding	
												Critical (kWh)	Non-critical (kWh)
1	11~15	4	7	3	5	8	9	6	2	10	1	3977.5	12930.0
2	11~15	4	7	3	5	8	6	10	2	1	9	3800.5	12978.0
3	11~15	4	7	3	6	8	5	10	2	1	9	3705.2	13175.8
4	11~15	10	4	5	3	2	7	6	8	1	9	3402.3	13756.8
5	11~15	10	4	5	3	9	6	2	7	1	8	3286.8	14212.0

C. *Superiority of the Co-Optimization Model*

The proposed co-optimization model is compared with the benchmark model which treats the DRM, MCDM and RCDM as three independent modelling problems. In this benchmark model, the MCDM is first solved by minimizing the time to repair all branches, and the repair time $A_k^{MC,RP}$ can be obtained as $A_k^{MC,RP*}$. Then, the repair time $A_k^{MC,RP*}$ is used as the input of DRM. The DRM minimizes the load curtailment with no consideration of the RCs' travel time and manual switches' operating time, and the travel path of RCs $x_{a,b,rc}^{RC}$ can be obtained as $x_{a,b,rc}^{RC*}$. Last, the travel path of RCs $x_{a,b,rc}^{RC*}$ is set as the input of RCDM, and the RCDM minimizes the travel time of RCs with the given routing path. The simulation results of the benchmark model are shown in Table VIII.

TABLE VIII LINE REPAIR AND ENERGIZATION SEQUENCE OF THE BENCHMARK MODEL

Time (min)	Line Repair	Switch-on Sequence		Cell energization
		Remote-controlled	Manual	
0				11,12,13,14,15
67	57-60			
90	60-62			
93	7-8			
117	109-110			
126	54-57			
132	76-86			
135	1-3			
136		149-150		1
196	101-105			
197		300-350		10
209	18-19			
219	44-47			
225	13-34			
233			1-7	2
247	67-160			
248	35-36			
259			151-300	5
275		450-451		7
288			13-152	6
313	89-91			
314		95-195		9
343			13-18	3
358	25-26			
359		250-251		4
403			76-77	8

In the benchmark model, the optimization objective of independent MCDM is to "minimize line outage duration". Hence, the damaged lines with less repair time are prioritized to be repaired, e.g., line 57-60 and 60-62. However, this repair scheme is not efficient for the load restoration. For example, line 57-60 in node cell 6 is first repaired at t =67min, but node cell 6 can only be energized at t=288min because 1) other damaged lines in node cell 6 (line 54-57 and 60-62) have not been repaired; 2) RCs have not arrived to the switch between node 13 and 152; and 3) node cell 6 is not prioritized in the DRM due to the lower priority of loads. Consequently, MCDM should be co-optimized with the DRM and RCDM to improve the load restoration efficiency.

Besides, the switching sequence and node cell energization sequence in the benchmark model are also suboptimal because the travel time and operating time of RCs are not considered in the DRM. In this case, RCs cannot timely attend manual switches to follow the switching sequence in DRM, which will further slow down the restoration process. Therefore, the RCDM is an essential part of the co-optimization model.

The superiority of the co-optimization model is demonstrated in Fig. 11, which compares the total restored power and energy by the proposed and benchmark models. Specifically, the proposed co-optimization model can restore power of all loads in 382min, which is 22min quicker than the benchmark model. Besides, the total power restored by co-optimization model is always higher than the benchmark model at any single point of time along the restoration process. Moreover, the co-optimization model can restore total energy of loads to 10463kWh, which is 41% higher than 7445kWh of the loads restored in the benchmark model.

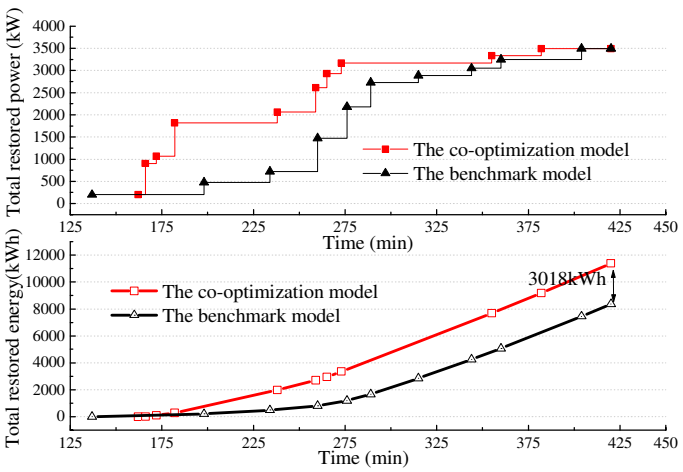

Fig.11. Comparison restored power and energy of loads.

The benchmark model may initially restore some loads quicker than the co-optimization model due to "minimize line outage duration" in the MCDM, as shown in the first 150 minutes of Fig. 11. However, the priority principle is generally conflicting with the "minimum load shedding" of DRM, thereby resulting in the restoration delay of node cells with

more loads (or critical loads), such as the node cell 5.

V. Conclusion

To enhance the resilience of power distribution systems, this paper proposes a novel co-optimization model for disaster recovery by integrating the maintenance and restoration crews dispatch. In the energization scheme, the MC dispatch, RC dispatch and switching sequence are co-optimized to improve the restoration efficiency. To address the time scale related challenges of DRM, MCDM and RCDM, the co-optimization problem is formulated as an "event-based" model with variable time steps. Moreover, the "Big-M" and "Small-ε" based linearization method is used to solve the co-optimization model as a MILP problem, and the clustering method is proposed to pre-assign damaged components to the nearest depots, both methods can reduce the computational complexity. The proposed co-optimization model is compared with the benchmark model which treats DRM, MCDM and RCDM independently. The numerical results demonstrate that the proposed method can efficiently improve the power and energy restoration of disconnected loads, and reduce the service restoration time of distribution systems.

References

[1] T. DiChristopher. Texas utilities struggle to restore power as Harvey hampers progress, Aug. 28, 2017. [Online]. Available: https://www.cnbc.com/2017/08/28/texas-utilities-struggle-to-restore-power-asharvey-hampers-progress.html

[2] P. Sullivan, M. Berman, and K. Zezima. After Irma, Florida preparesfor days-and maybe weeks-without power, Sep. 13, 2017. [Online]. Available:https://www.washingtonpost.com/news/postnation/wp/2017/09/12/florida-struggles-with-top-job-in-irmas-wakerestoring-power-to-millions

[3] Y. Xu, C. Liu, K. P. Schneider, and D. T. Ton, "Toward a resilient distribution system," in *Proc. IEEE Power Energy Soc. Gen. Meeting*, Denver, CO, USA, 2015, pp. 1–5.

[4] National Academies of Sciences, Engineering and Medicine, Enhancing the Resilience of the Nation's Electricity System, Washington, DC: The National Academies Press, 2017.

[5] Y. Xu, C. Liu, K. P. Schneider, F. K. Tuffner and D. T. Ton, "Microgrids for Service Restoration to Critical Load in a Resilient Distribution System," *IEEE Trans. Smart Grid*, vol. 9, no. 1, pp. 426-437, Jan. 2018.

[6] H. Gao, Y. Chen, Y. Xu and C. Liu, "Resilience-Oriented Critical Load Restoration Using Microgrids in Distribution Systems," *IEEE Trans. Smart Grid*, vol. 7, no. 6, pp. 2837-2848, Nov. 2016.

[7] C. Chen, J. Wang, F. Qiu and D. Zhao, "Resilient Distribution System by Microgrids Formation After Natural Disasters," *IEEE Trans. Smart Grid*, vol. 7, no. 2, pp. 958-966, March 2016.

[8] Z. Wang, C. Shen, Y. Xu, F. Liu, X. Wu and C. Liu, "Risk-Limiting Load Restoration for Resilience Enhancement With Intermittent Energy Resources," *IEEE Trans. Smart Grid*, vol. 10, no. 3, pp. 2507-2522, May 2019.

[9] S. Yao, P. Wang and T. Zhao, "Transportable Energy Storage for More Resilient Distribution Systems With Multiple Microgrids," *IEEE Trans. Smart Grid*, vol. 10, no. 3, pp. 3331-3341, May 2019.

[10] A. Arif, Z. Wang, J. Wang and C. Chen, "Power Distribution System Outage Management With Co-Optimization of Repairs, Reconfiguration, and DG Dispatch," *IEEE Trans. Smart Grid*, vol. 9, no. 5, pp. 4109-4118, Sept. 2018.

[11] A. Arif, S. Ma, Z. Wang, J. Wang, S. M. Ryan and C. Chen, "Optimizing Service Restoration in Distribution Systems With Uncertain Repair Time and Demand," *IEEE Trans. Power Syst.*, vol. 33, no. 6, pp. 6828-6838, Nov. 2018.

[12] S. Lei, C. Chen, Y. Li and Y. Hou, "Resilient Disaster Recovery Logistics of Distribution Systems: Co-Optimize Service Restoration with Repair Crew and Mobile Power Source Dispatch," *IEEE Trans. Smart Grid*. doi: 10.1109/TSG.2019.2899353

[13] M. S. Khomami, M. S. Sepasian, "Pre-hurricane optimal placement model of repair teams to improve distribution network resilience," *Elect. Power Syst. Res.*, vol. 165, pp. 1-8, 2018

[14] B. Chen, C. Chen, J. Wang and K. L. Butler-Purry, "Multi-Time Step Service Restoration for Advanced Distribution Systems and Microgrids," *IEEE Trans. Smart Grid*, vol. 9, no. 6, pp. 6793-6805, Nov. 2018.

[15] C. Chen, J. Wang, and D. Ton, "Modernizing Distribution System Restoration to Achieve Grid Resiliency Against Extreme Weather Events: An Integrated Solution," *Proceedings of the IEEE*, vol. 105, no. 7, pp. 1267-1288, 2017.

[16] S. Toune, H. Fudo, T. Genji, Y. Fukuyama, and Y. Nakanishi, "Comparative study of modern heuristic algorithms to service restoration in distribution systems," *IEEE Trans. Power Del.*, vol. 17, no. 1, pp. 173-181, 2002.

[17] Z. Qin, D. Shirmohammadi, and W. H. E. Liu, "Distribution feeder reconfiguration for service restoration and load balancing," *IEEE Trans. Power Syst.,* vol. 12, no. 2, pp. 724-729, 1997.

[18] C. Chao-Shun, L. Chia-Hung, and T. Hung-Ying, "A rule-based expert system with colored Petri net models for distribution system service restoration," *IEEE Trans. Power Syst.*, vol. 17, no. 4, pp. 1073-1080, 2002.

[19] B. Chen, Z. Ye, C. Chen and J. Wang, "Toward a MILP Modeling Framework for Distribution System Restoration," *IEEE Trans. Power Syst.,* vol. 34, no. 3, pp. 1749-1760, May 2019.

[20] B. Chen, C. Chen, J. Wang and K. L. Butler-Purry, "Sequential Service Restoration for Unbalanced Distribution Systems and Microgrids," *IEEE Trans. Power Syst.*, vol. 33, no. 2, pp. 1507-1520, March 2018.

[21] Y. Xu, C. Liu, K. P. Schneider and D. T. Ton, "Placement of Remote-Controlled Switches to Enhance Distribution System Restoration Capability," *IEEE Trans. Power Syst.*, vol. 31, no. 2, pp. 1139-1150, March 2016.

[22] M. E. Baran and F. F. Wu, "Network reconfiguration in distribution systems for loss reduction and load balancing," *IEEE Trans. Power Del.*, vol. 4, no. 2, pp. 1401–1407, Apr. 1989.

[23] A. Arif and Z. Wang, "Networked microgrids for service restoration in resilient distribution systems," *IET Gener. Transm. Distrib.,* vol. 11, no. 14, pp. 3612-3619, 2017.

[24] A. Arif, S. Ma, Z. Wang, J. Wang, S. M. Ryan and C. Chen, "Optimizing Service Restoration in Distribution Systems With Uncertain Repair Time and Demand," *IEEE Trans. Power Syst.*, vol. 33, no. 6, pp. 6828-6838, Nov. 2018.

[25] K. P. Schneider, E. Sortomme, S. S. Venkata, M. T. Miller, and L. Ponder, "Evaluating the magnitude and duration of cold load pick-up on residential distribution using multi-state load models," *IEEE Trans. Power Syst.*, vol. 31, no. 5, pp. 3765–3774, Sep. 2016.

[26] X. Lu, K. W. Chan, S. Xia, X. Zhang, G. Wang and F. Li, "A Model to Mitigate Forecast Uncertainties in Distribution Systems Using the Temporal Flexibility of EVAs," *IEEE Trans. Power Syst.*, vol. 35, no. 3, pp. 2212-2221, May 2020.

[27] C. J. Zapata, S. C. Silva, and O. L. Burbano, "Repair models of power distribution components," in Proc. IEEE/PES Transm. and Distrib. Conf. and Expo.: Latin America, Bogota, Colombia, Aug. 2008, pp. 1–6.

[28] Jin Zhao, Yao Liu, Hongtao Wang, Qiuwei Wu, "Receding horizon load restoration for coupled transmission and distribution system considering load-source uncertainty," *International Journal of Electrical Power & Energy Systems*, Vol.116, 2020.

[29] Y. Zhang, J. Wang and J. Liu, "Attack Identification and Correction for PMU GPS Spoofing in Unbalanced Distribution Systems," *IEEE Trans. Smart Grid*, vol. 11, no. 1, pp. 762-773, Jan. 2020.

[30] N. G. Bretas, S. A. Piereti, A. S. Bretas and A. C. P. Martins, "A Geometrical View for Multiple Gross Errors Detection, Identification, and Correction in Power System State Estimation," *IEEE Trans. Power Systems*, vol. 28, no. 3, pp. 2128-2135, Aug. 2013.

[31] P. Demetriou, M. Asprou and E. Kyriakides, "A Real-Time Controlled Islanding and Restoration Scheme Based on Estimated States," IEEE Trans. Power Systems, vol. 34, no. 1, pp. 606-615, Jan. 2019.

[32] IEEE PES Power System Analysis, Computing, and Economics Committee. (Feb. 2014). IEEE 123 Node Test Feeder. [Online].Available: http://ewh.ieee.org/soc/pes/dsacom/testfeeders/feeder123.zip

Gang Zhang (S'18) received the B.Sc. degree in electrical engineering in 2016 from Shandong University, Jinan, China, where he is currently working toward the Ph.D. degree in electrical engineering. His research interests include multi-energy system, power system resilience, distribution system planning, and power system optimization.

Feng Zhang (M'11) received his Ph.D. degree from Shandong University, China, in 2011. He is currently with School of Electrical Engineering, Shandong University, Jinan, China. During 2015 and 2016, he was a Research Associate at Department of Electrical Engineering, The Hong Kong Polytechnic University. In 2017, he was a visiting scholar at the School of Electrical and Information Engineering, The University of Sydney, Sydney, NSW, Australia. His research interests include renewable energy and energy storage.

Xin Zhang (M'16, SM'19) received the B.Eng. degree in automation from Shandong University, China, in 2006; the M.Sc. and Ph.D. degrees in electrical power engineering from The University of Manchester, U.K., in 2007 and 2010 respectively.
He is an Associate Professor (Senior Lecturer) in energy systems at Cranfield University, U.K. He was a Power System Engineer in the Electricity National Control Centre at the National Grid, U.K. His research and industrial experience include power system planning and operation, renewable energy integration, and multi-energy systems. He is a Chartered Engineer with the U.K. Engineering Council.

Ke Meng (M'10, SM'19) received the Ph.D. degree in electrical engineering from the University of Queensland, Brisbane, QLD, Australia, in 2009. He is currently a Senior Lecturer with the School of Electrical Engineering and Telecommunications, The University of New South Wales, Sydney, NSW, Australia. He was previously a Lecturer with the School of Electrical and Information Engineering, The University of Sydney, Sydney, NSW, Australia. His research interests include pattern recognition, power system stability analysis, and wind power and energy storage.

Zhao Yang Dong (M'99–SM'06–F'17) received the Ph.D. degree from the University of Sydney, Sydney, Australia, in 1999. He is currently the SHARP Professor with the University of New South Wales, the Director of ARC Research Hub for Integrated Energy Storage Solutions, and the Director of UNSW Digital Grid Futures Institute, Sydney, NSW, Australia. He was previously a Professor and the Head of the School of Electrical and Information Engineering, The University of Sydney, and the Ausgrid Chair and the Director of the Centre for Intelligent Electricity Networks, University of Newcastle, Callaghan, NSW, Australia. He also held industrial positions with Transend Networks (now TAS Networks), Australia. His research interests include smart grid, power system planning, power system security, load modeling, electricity market, and computational intelligence and its application in power engineering. He is an Editor for the IEEE TRANSACTIONS ON SMART GRID, IEEE TRANSACTIONS ON SUSTAINABLE ENERGY, IEEE POWER ENGINEERING LETTERS, and *IET Renewable Power Generation*.